



## Effect of the applied stress and the friction stress on the dislocation dissociation in face centered cubic metals

Q1 Jean-Baptiste Baudouin<sup>a,b</sup>, Ghiath Monnet<sup>a,\*</sup>, Michel Perez<sup>b</sup>, Christophe Domain<sup>a</sup>, Akiyoshi Nomoto<sup>c</sup>

<sup>a</sup> EDF—Centre de Recherche des Renardières, 77250 Moret sur Loing, France

<sup>b</sup> Université de Lyon, INSA Lyon, MATEIS—UMR CNRS 5510, F69621 Villeurbanne, France

<sup>c</sup> Central Research Institute of Electric Power Industry, 2-11-1 Iwado Kita, Komae-shi, Tokyo 201-8511, Japan

### ARTICLE INFO

#### Article history:

Received 27 September 2012

Accepted 29 October 2012

#### Keywords:

Dislocation  
Dissociation  
FCC metals  
Plasticity

### ABSTRACT

The separation between partials in face-centered-cubic (FCC) alloys is known to be a function of the elastic constants and the stacking fault energy (SFE). In this work, we complete this classical picture by investigating three other effects. First we show that the applied stress component in the slip plane perpendicular to the Burgers vector induces an additional force on the partials. Depending on the value of the SFE, a critical value for this shear component leads to an infinite separation, which explains the deformation mechanism by formation of extended stacking faults. In alloys where the friction stress is not negligible, we show that the friction plays an important and complex role on dissociation, depending on the previous dislocation motion. This factor can be responsible for the discrepancy in experimental measurement of the dissociation width. In all cases, we show that the effect of the friction stress vanishes as soon as the dislocation starts gliding in its slip plane. Finally, we show that the choice of effective shear modulus in elastically anisotropic materials constitutes an important feature in the determination of the equilibrium dissociation width.

© 2012 Published by Elsevier B.V.

### 1. Introduction

The dislocation dissociation is an important feature in low SFE materials such as AISI 316 type austenitic stainless steels [1,2]. The dissociation is supposed to be the controlling factor in the formation of twins and extended stacking faults [3,4]. Large numbers of experimental investigations report on the activation of these mechanisms in the 316L steels (see for example [5,6]).

Recently, Byun [7] investigated the role of the applied stress on the partial separation and showed that some stress components may be responsible for the spreading of stacking faults, affecting substantially the deformation microstructure.

In these investigations, an implicit assumption is made: the friction stress on the Shockley partials is considered to be negligible. In the case of pure FCC metals, this assumption is quite plausible, since the critical resolved shear stress measured on single crystals is very low. However, in industrial materials made harder by alloying, this assumption may be questionable.

In this paper, we investigate theoretically the role of the applied stress as well as the friction stress on the dissociation spacing. Unlike the convention considered by Byun [7], we consider a configuration in which a stress tensor is applied to a

crystal containing a slip system with a fixed Burgers vector and slip plane. The dissociation distance is studied as a function of the dislocation character, *i.e.* the angle made by the dislocation line and its Burgers vector. The force balance includes the presence of a friction stress on every Shockley partial. For the sake of simplicity, we consider here the mathematical derivation of an isotropic material, which makes sense when we consider that in Discrete Dislocation Dynamics a wide range of codes are based on the isotropy concept. Thus we then make an application on the case of the 316L steel and we discuss the effect of friction stress and the choice of the effective isotropic elastic constants on the dissociation width.

### 2. Force components

Consider a perfect dislocation with a line vector parallel to the  $\vec{e}_r$  axis of a cylindrical coordinate system, incorporated in a Cartesian coordinate system as shown in Fig. 1. The orthonormal Cartesian axes coincide with the crystal axes:  $\vec{e}_x = (1/\sqrt{2})[\bar{1} \ 1 \ 0]$ ,  $\vec{e}_y = (1/\sqrt{6})[\bar{1} \ \bar{1} \ 2]$  and  $\vec{e}_z = (1/\sqrt{3})[\bar{1} \ 1 \ 1]$ . The dislocation Burgers vector is  $\vec{b} = (1/2)[\bar{1} \ 1 \ 0]$  and can be written as  $\vec{b} = b\vec{e}_x$ . The normal to the slip plane matches with the z-axis of our coordinate. The dislocation character refers to the angle  $\theta$  between the dislocation line vector  $\vec{e}_r$  and the Burgers vector. In order to study the influence of the applied stress tensor on the

\* Corresponding author.

E-mail address: [ghiath.monnet@edf.fr](mailto:ghiath.monnet@edf.fr) (G. Monnet).

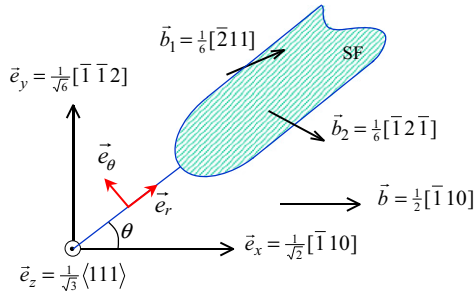


Fig. 1. Configuration of the perfect and dissociated dislocations.

dissociation of a dislocation loop in a given slip system, the dislocation Burgers vector should be kept constant while the angle  $\theta$  varies from 0 (screw dislocation) to 90° (edge dislocation). This change in the dislocation character differs from that considered by Byun [7], who fixed the dislocation line vector and considered a rotation of the Burgers vector in the slip plane, which leads to a rotation in comparison with the stress coordinate system. We believe that the Burgers vector of the slip system should be fixed in the crystal coordinate system for two reasons: (i) the direction of the Burgers vector cannot rotate freely since it must match with the dense crystallographic direction and (ii) along a dislocation loop the Burgers vector is constant while the dislocation line vector varies.

According to the elastic theory of dislocations [3], the perfect dislocation described above tends to dissociate into Shockley partials as sketched in Fig. 1. We consider the dissociation plane to be the  $x$ - $y$  plane. The leading partial is given by  $\vec{b}_1 = [\alpha\beta 0]$ , while the trailing partial is  $\vec{b}_2 = [\alpha - \beta 0]$ , where  $\alpha$  equals  $(a\sqrt{2}/4)$  and  $\beta$  equals  $(a\sqrt{6}/12)$  and  $a$  is the lattice parameter. With these variables, the Burgers vector becomes  $\vec{b} = [2\alpha 0 0]$ . In order to investigate the effects of all stress components, we consider the general stress tensor  $\Sigma$  written in our Cartesian coordinate system:

$$\Sigma = \begin{pmatrix} \sigma_{xx} & \tau_{xy} & \tau_{xz} \\ \tau_{xy} & \sigma_{yy} & \tau_{yz} \\ \tau_{xz} & \tau_{yz} & \sigma_{zz} \end{pmatrix} \quad (1)$$

Given the configuration considered in Fig. 1, the resultant forces per unit length on the leading partial is given by

$$\vec{F}_1 = \vec{F}_{int} - \gamma \vec{e}_\theta + \vec{F}_{PK,1} + \varepsilon_1 F_f \vec{e}_\theta \quad (2)$$

This balance of forces is equivalent to the one presented by Hirth and Lothe [3], except that in this study the force components are more detailed. The different forces appearing on the right-hand side are, correspondingly the interaction force with the trailing partial, the attractive force resisting the expansion of the stacking fault, the Peach-Koehler force [8] and the friction force:  $F_f = b\tau_f$ , where  $\tau_f$  is the friction stress.  $\varepsilon_1$  is a sign parameter ( $\varepsilon_1 = \pm 1$ ) depending on the direction of motion of the leading partial. Equivalently, the effective stress on the trailing partial can be given as

$$\vec{F}_2 = \vec{F}_{int} + \gamma \vec{e}_\theta + \vec{F}_{PK,2} + \varepsilon_2 F_f \vec{e}_\theta \quad (3)$$

Note that since the crystallographic nature of the two partials is different, there is no evidence that both friction forces are equal. However, for the sake of simplicity we consider that the difference between them is negligible. Projecting these forces on the  $\vec{e}_\theta$  axis, we get

$$F_1 = \vec{F}_1 \cdot \vec{e}_\theta = F_{int} - \gamma + F_{PK,1} + \varepsilon_1 F_f \quad (4)$$

for the leading partial and

$$F_2 = \vec{F}_2 \cdot \vec{e}_\theta = -F_{int} + \gamma + F_{PK,2} + \varepsilon_2 F_f \quad (5)$$

for the trailing partial. Using the classical formulas for the Peach-Koehler force [8], one finds

$$F_{PK,1} = \alpha\tau_{xz} + \beta\tau_{yz} \quad (6)$$

and

$$F_{PK,2} = \alpha\tau_{xz} - \beta\tau_{yz} \quad (7)$$

As expected, only the stress component parallel to each Burgers vector component contributes to the effective force on every partial. On the other hand, the interaction force per unit length between the parallel partials can be computed using Eq. (5.17) of Hirth and Lothe textbook [3], which was first developed by Nabarro [9]. In our case, we have

$$F_{int} = \frac{G}{2\pi d} \left[ (\alpha^2 + \beta^2) \cos^2 \theta - \beta^2 + \frac{\alpha^2 \sin^2 \theta - \beta^2 \cos^2 \theta}{1-\nu} \right] \quad (8)$$

where  $G$  is the shear modulus and  $d$  the spacing between partials. Since  $\alpha^2$  and  $\beta^2$  equal respectively  $(b^2/4)$  and  $(b^2/12)$ ,  $F_{int}$  can be reduced to

$$F_{int} = \frac{Gb^2}{24\pi(1-\nu)d} (2 + \nu - 4\nu \cos^2 \theta) \quad (9)$$

### 3. Equilibrium at zero applied stress

When  $\tau_{xz}$  and  $\tau_{yz}$  vanish, one can identify the equilibrium dissociation distance. The energy of the dissociated dislocation  $E(d)$  must exhibit a minimum for the equilibrium spacing  $d = d_0$ . If every partial is shifted away from the other one by  $dx$ , the associated change in energy is given by  $\Delta E = F_1 dx - F_2 dx$ . Since at equilibrium  $\Delta E$  must vanish, we have  $2F_{int} - 2\gamma + \varepsilon_1 F_f - \varepsilon_2 F_f = 0$ . The parameters  $\varepsilon_i$  depend on the direction of motion of every partial dislocation towards the equilibrium position. Two important cases can be distinguished. If the partials move away from each other towards the equilibrium dissociation distance  $d_0$ , then  $\varepsilon_1$  is equal  $-1$  and  $\varepsilon_2$  is equal  $+1$  and the separation distance reached is

$$d_1^0 = \frac{2 + \nu - 4\nu \cos^2 \theta}{24\pi(1-\nu)} \frac{Gb^2}{\gamma + F_f} \quad (10)$$

In the other case where the dissociation tends to shrink from larger dissociation distance, partials move towards each other and  $\varepsilon_1$  is now equal to  $+1$  and  $\varepsilon_2$  is  $-1$ . We then have

$$d_2^0 = \frac{2 + \nu - 4\nu \cos^2 \theta}{24\pi(1-\nu)} \frac{Gb^2}{\gamma - F_f} \quad (11)$$

The presence of a friction force causes a degeneration of the dissociation distance depending on the direction of motion of the partials.

### 4. Dissociation under applied stress

Only the applied shear components  $\tau_{xz}$  and  $\tau_{yz}$  contribute to the force on the partial dislocations. The sum of the two forces corresponds to the net force  $F_{tot}$  on the perfect dislocation, i.e. on the ensemble of the two partials. Depending on the sign and amplitude of the non-friction part of  $F_1$  and  $F_2$ , namely

$$F_1^{nf} = F_{int} - \gamma + F_{PK,1} \quad (12)$$

$$F_2^{nf} = -F_{int} + \gamma + F_{PK,2} \quad (13)$$

**Table 1**  
Displacement scenarios for each partial and associated value of  $\varepsilon_{1,2}$  and/or  $F_{1,2}$ .

| Partial | Condition               | $\varepsilon_{1,2}$  | Action                        |
|---------|-------------------------|----------------------|-------------------------------|
| 1       | $F_1^{nf} > F_f$        | $\varepsilon_1 = -1$ | Displ. twds $\vec{e}_\theta$  |
|         | $-F_f < F_1^{nf} < F_f$ | $F_1 = 0$            | Partial 1 pinned              |
| 2       | $F_2^{nf} < -F_f$       | $\varepsilon_1 = +1$ | Displ. twds $-\vec{e}_\theta$ |
|         | $F_2^{nf} > F_f$        | $\varepsilon_2 = -1$ | Displ. twds $\vec{e}_\theta$  |
|         | $-F_f < F_2^{nf} < F_f$ | $F_2 = 0$            | Partial 2 pinned              |
|         | $F_2^{nf} < -F_f$       | $\varepsilon_2 = +1$ | Displ. twds $-\vec{e}_\theta$ |

three possible scenarios per partial can occur: it can move backward, forward or be pinned (see Table 1).

**5. Discussion**

We discuss our results in light of application on the 316L steel, which is of technological interest in nuclear industry. The single crystal elastic constants are  $C_{11}=210$  GPa,  $C_{12}=130$  GPa,  $C_{44}=120$  GPa [10]. The application of our theoretical results on this material faces two difficulties: (i) the material is highly anisotropic and (ii) the SFE varies substantially between the different alloys from 10 to 40 mJ/m<sup>2</sup> [2]. For the sake of simplification, we treat three sets of effective isotropic elastic constants: the Voigt average [11] ( $G=88$  GPa,  $\nu=0.26$ ), the Reuss average [12] ( $G=60$ ,  $\nu=0.32$ ) and the Scattergood and Bacon average [13,14] ( $G=61$ ,  $\nu=0.4$ ).

In the absence of applied stress and depending on the considered effective elastic constants, we get different values for the friction-free material concerning the screw ( $\theta=0^\circ$ ) and edge ( $\theta=90^\circ$ ) perfect dislocations. Depending on the material and the elastic constants to be considered, the dissociation of screw dislocations varies from 1.7 to 11.8 nm, while that of edge dislocations varies from 4.2 to 21.9 nm.

Depending on the average considered, the dissociation distance for the screw dislocation varies by almost a factor of two, while that of the edge dislocations changes only by 30%. Increasing the SFE by a factor of 4 causes the dissociation distance to decrease by a factor of 4.

In the presence of applied stress, the stress component parallel to the perfect Burgers vector, i.e.  $\tau_{xz}$  in our configuration, contributes to a global motion of the two partials in the same direction. However, the presence of a shear stress component perpendicular to the perfect Burgers vector leads to a change in separation distance. In the configuration of Fig. 1, a negative value of  $\tau_{yz}$  enhances the effect of the SFE, while a positive value of  $\tau_{yz}$  causes the stacking fault to extend. Escaig stress had to be introduced right at the time when we defined it [17]. But in this study, we are not considering the effect of curvature.

The dissociation distance has been evaluated as a function of  $\tau_{xz}$  and  $\tau_{yz}$  (see Fig. 2). The friction force  $F_f=b\tau_f$  with  $\tau_f=90$  MPa has been used in this paper, in agreement with molecular dynamics simulations performed on a Fe-Ni-Cr alloy [16].

Depending on the applied stress, three domains are observed on Fig. 2

- 1)  $F_1=F_2=0$  (in a diamond shaped domain delimited by  $|\alpha\tau_{xy} + \beta\tau_{yz}| < b\tau_f$  and  $|\alpha\tau_{xy} - \beta\tau_{yz}| < b\tau_f$ ), both partials are pinned by the friction force and thus remain immobile;
- 2) one (or two) partial(s) is (are) pinned and the dissociation distance tends to an equilibrium value;
- 3) one (or two) partial(s) is (are) unpinned and the dissociation distance diverges to infinity.

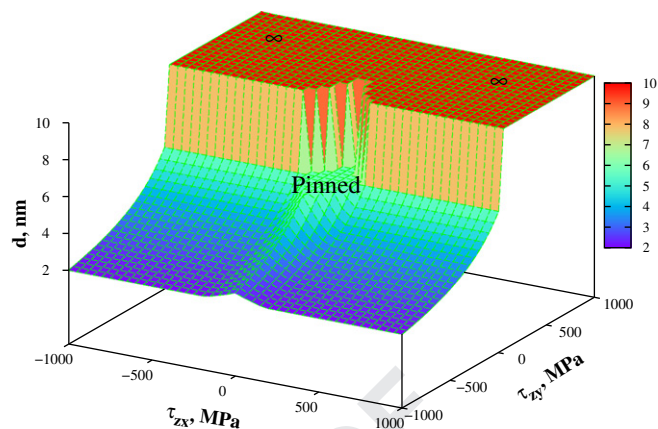


**Fig. 2.** Typical surface of dissociation distance between both partials for different values of stresses in the ( $\tau_{xz}$ ,  $\tau_{yz}$ ) plane. Friction force has been set to  $\tau_f=90$  MPa ( $F_f=b\tau_f$ ) [16]. Voigt average for the effective isotropic elastic constants has been considered (see text).

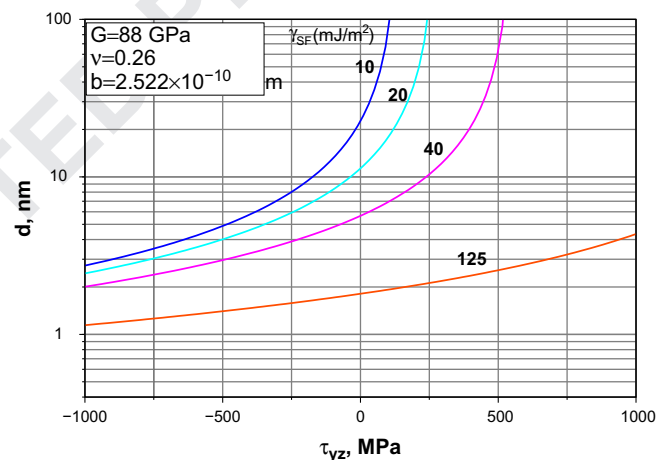


**Fig. 3.** Partial separation distance versus stress component  $\tau_{yz}$  for different SFE values  $\gamma$  (edge character). Voigt average for the effective isotropic elastic constants has been considered (see text).

In the case where both partials are moving in the same direction (thanks to the contribution of  $\tau_{xz}$ ), we have  $\varepsilon_1=\varepsilon_2 = \pm 1$ . Thus, at dynamical equilibrium, the dissociation distance is such that the force acting on both partials is equal:  $F_1=F_2$ , leading to the dissociation distance

$$d_\tau = \frac{2 + \nu - 4\nu\cos^2\theta}{24\pi(1-\nu)} \frac{Gb^2}{\gamma - \beta\tau_{yz}} \quad (14)$$

It is remarkable that the separation  $d_\tau$  between partials becomes independent of the friction stress and the  $\tau_{xz}$  shear stress component. Moreover, for a critical value  $\tau_{yz,c}=\gamma/\beta$ , the partial separation becomes infinite for screw dislocations as well as for edge dislocations. This conclusion is different from that drawn by Byun [7], who stated that dissociation distance diverges only for screw dislocations. This difference is due to (i) the evolution of the stress state with the dislocation line orientation: in Byun's paper, the dislocation line was fixed whereas the orientation of the Burgers vector varied (which is a surprising choice); and (ii) Byun only considered  $\tau_{xz}$  to be non-zero, whereas it has been shown here that  $\tau_{yz}$  contributes to the partials divergences.

The evolution of the dissociation distance *versus* shear stress component  $\tau_{yz}$  is presented in Fig. 3 for different value of SFE. For the reference 316L material,  $\tau_{yz, c}$  varies between 100 MPa (for  $\gamma = 10 \text{ mJ/m}^2$ ) and 500 MPa (for  $\gamma = 40 \text{ mJ/m}^2$ ). For Nickel ( $\gamma = 125 \text{ mJ/m}^2$ ), it is not possible to evaluate  $\tau_{yz, c}$  in this stress range. As discussed by Byun [7] these stress levels can be easily met during deformation of austenitic steels [1] and are frequently reached in mechanical tests [2,15]. In this case, partial dislocations are expected to move separately, thus, inducing extended faults and facilitating twin formations.

## 6. Conclusion

Theoretical analysis of the effect of the stress on the separation distance of partial dislocations has been investigated. The results obtained in this article are summarised as follows:

- 1) A global expression has been established gathering the different forces exerted on dislocation partials. The stress acting on the dislocation is introduced using the Peach–Kœhler formula. The partials experience attractive and repulsive forces, which are introduced via the SFE, the Nabarro Formula and the Peach–Kœhler formula.
- 2) It is shown that only two stress components  $\tau_{xz}$  and  $\tau_{yz}$  affect the dislocation:  $\tau_{xz}$  leads to the movement of the whole dislocation whereas  $\tau_{yz}$  influences the dissociation distance.
- 3) Above a critical stress  $\tau_{yz}$ , which depends only on the SFE, it is found that the distance between the two partials diverges, whatever the dislocation type (edge or screw).

- 4) The friction stress on partial dislocations is found to affect strongly the dissociation width. Depending on the previous motion of the dislocation this stress may retain the partials far from their equilibrium spacing.

## Acknowledgement

This work is partially supported by the European FP7 Project PERFORM60. Details on this project can be found on [www.PERFORM.net](http://www.PERFORM.net).

## References

- [1] Lo K, Shek C, Lai J. Mater Sci Eng R: Rep 2009;65:39–104.
- [2] Li X, Almazouzi A. J Nucl Mater 2009;385:329–33.
- [3] Hirth JP, Lothe J. Theory of dislocations. Krieger Publishing Company; 1982.
- [4] Hull D, Bacon DJ. Introduction to dislocations. Butterworth-Heinemann; 2001.
- [5] Feaugas X. Acta Mater 1999;47:3617–32.
- [6] Lee E, Byun T, Humm J, Yoo M, Farrell K, Mansur L. Acta Mater 2001;49:3269–76.
- [7] Byun T. Acta Mater 2003;51:3063–71.
- [8] Peach M, Kœhler JS. Phys Rev 1950;80:436–9.
- [9] Nabarro FRN. Adv Phys 1952;1:269–394.
- [10] Mangalick ME, Fiore NF. Trans Metall Soc AIME 1968;242:2363–4.
- [11] Voigt W. Lehrbuch der Kristalphysik. Teubner; 1928.
- [12] Reuss A. Z Angew Math Mech 1929;9:49–58.
- [13] Scattergood RO, Bacon DJ. Phys Status Solidi A 1974;25:395–404.
- [14] Bacon DJ. In: Bilby BA, Miller KJ, Jr. JRW, editors. Fundamentals of deformation and fracture. Eshelby memorial symposium. Cambridge, England; Sheffield, England: Cambridge University Press; 1985.
- [15] Byun T, Hashimoto N, Farrell K. Acta Mater 2004;52:3889–99.
- [16] Bonny G, Terentyev D, Pasianot RC, Ponce S, Bakaev A. Model Simul Mater Sci Eng 2011;19:085008.
- [17] Escaig B. J Phys 1968;29:225–39.